

component is positive and the excited hydrogen atom should dissociate along the direction of the electron beam. While the $(1b_1)$ orbital is nonbonding, the $(3a_1)$ orbital is bonding to the O-H bond and tends to hold two hydrogen atoms closer; the removal of an electron from the $(3a_1)$ orbital expands the H-O-H bond angle wider and the water molecule approaches a linear structure.³⁵ Thus, the dissociation from the $(3a_1)^{-1}(1b_1)^{-1}-(4a_1)^1(nR)^1$ state could be parallel to the direction of the transition moment and to that of the electron beam at low electron energies as shown in Figure 6. Since the observed value of β is positive, the symmetry of the Rydberg states would be B_2 . Because the symmetry of the core ion is B_1 , the symmetry of the Rydberg orbital should be A_2 .

The third component is also a fast component; its translational energy is mainly at 2-6 eV. It has been concluded¹² that this component has a threshold at 31.3 eV and that its formation is a direct dissociation to three fragments ($H^* + H + O$) through the Rydberg states converging to the ${}^2A_1(2a_1)^{-1}$ state of H_2O^+ .

(35) Turner, D. W.; Baker, C. B.; Baker, A. D.; Brundle, C. R. *Molecular Photoelectron Spectroscopy*; John Wiley & Sons: London, 1970; Chapter 4.3.

Tan et al. indicated that formation of a proton through the ${}^2A_1(2a_1)^{-1}$ state has a threshold at about 28 eV and an onset at about 32 eV.²¹ Kurawaki et al.¹² may have missed a threshold at about 27 eV, since it is a weak one. There is some satellite structure around the 2A_1 state,²³ and the Rydberg states converging to them may also be intermediate states for the formation of this component. Anisotropy is small in the formation of this component, and the asymmetry parameter, β , of this component is slightly negative. This finding indicates that the symmetry of the Rydberg states would be A_1 . This is identical with the core ion, and thus the symmetry of the Rydberg orbital should also be A_1 .

The fourth component is very fast. Formation of this component should proceed through some doubly excited states of H_2O , and an ionic species is produced in addition to H^* at its dissociation limit.

Acknowledgment. This work is partially supported by a Grant-in-Aid for Scientific Research on Priority Areas (62606519, 63606512, 01606002) from the Ministry of Education, Science and Culture.

Registry No. H_2O , 7732-18-5; H, 12385-13-6.

Correlation of Infrared and UV-Visible Bands of Matrix-Isolated Carbon Clusters

Jan Szczepanski and Martin Vala*

Department of Chemistry, University of Florida, Gainesville, Florida 32611-2046
(Received: September 26, 1990)

Carbon clusters, formed by Nd:YAG laser ablation of graphite, have been trapped in solid argon at 12 K. Using Fourier transform infrared and UV-visible spectrometers in a crossed beam configuration we have recorded the IR and UV-visible absorption spectra of the same carbon/Ar matrix and followed the growth and decay of bands in both regions as a function of matrix annealing temperature and initial preparation conditions. For the IR bands at 2164 and 1998 cm^{-1} , previously attributed to linear C_5 and nearly linear C_8 clusters, respectively, good correlations have been found with the 223- and 308-nm bands, respectively. The 2164- cm^{-1} /223-nm correlation represents the first positive assignment for an electronic band due to C_5 . The similarity of the 223-nm band system with the so-called 217.5-nm interstellar "hump" has been noted and it is suggested that linear C_5 clusters may be responsible for this much-discussed feature. Good correlations were also found for the 2039- cm^{-1} /283-nm, 2039- cm^{-1} /410-nm, and 1695- cm^{-1} /586-nm pairs. The 2039- cm^{-1} /410-nm bands are known to originate from C_3 , while the species responsible for the 1695- cm^{-1} /586 nm pair is suggested to be a cyclic cluster of six or more carbons. A prominent UV band system at 247.1 nm has been correlated with an IR band at 2004 cm^{-1} and tentatively assigned to linear C_9 .

I. Introduction

There is much current interest in the clusters of carbon, particularly because of their apparent importance in astrophysics, soot formation, and flame chemistry. Much effort has been expended on both theoretical and experimental fronts in learning about these fascinating species.¹ To date the greatest fraction of this effort has been directed toward gaining an understanding of the *ground-state* properties of the carbon clusters: their most stable geometries and multiplicities, their thermodynamic properties, and their vibrational frequencies. Neutral and ionic clusters containing two or three carbons have been studied in greater detail than the larger clusters, but even with these species much still remains to be learned.¹

Several studies have been reported²⁻⁴ on the excited electronic transitions of clusters containing more than three carbons. Early work by Weltner and McLeod² focused on C_2 and C_3 but presented UV-visible (and IR) spectra observed after matrix annealing. The new bands were attributed to higher polycarbons, such as C_4 , C_5 , etc. Krättschmer and co-workers³ observed the UV-visible spectra

of matrix-isolated carbon clusters produced by resistively heating a graphite rod and tentatively assigned the prominent bands to linear carbon chains from C_4 to C_9 . Recently, Kurtz and Huffman⁴ reported on a study in which the UV-visible and infrared spectra were measured on the same matrix sample and studied as a function of annealing temperature. A good correlation was discovered between the 308-nm electronic band and the 1998- cm^{-1} vibrational band.

In the present paper we report the results of our study on the combined infrared/UV-visible spectra of a number of carbon clusters. The approach used in our work is similar to that pioneered by Kurtz and Huffman.⁴ We have, however, used laser ablation to form the clusters and were able to obtain higher

(1) For a recent review, cf.: Weltner, Jr., W.; Van Zee, R. *J. Chem. Rev.* **1989**, *89*, 1713.

(2) Weltner, Jr., W.; McLeod, Jr., D. *J. Chem. Phys.* **1966**, *45*, 3096.

(3) Krättschmer, W.; Sorg, N.; Huffman, D. *Surf. Sci.* **1985**, *156*, 814. Krättschmer, W.; Nachtigal, K. In *Polycyclic Aromatic Hydrocarbons and Astrophysics*; Léger, A., d'Hendecourt, L., Eds.; NATO-ASI Series; D. Reidel: Dordrecht, 1987.

(4) Kurtz, J.; Huffman, D. *J. Chem. Phys.* **1990**, *92*, 30.

* Author to whom correspondence should be addressed.

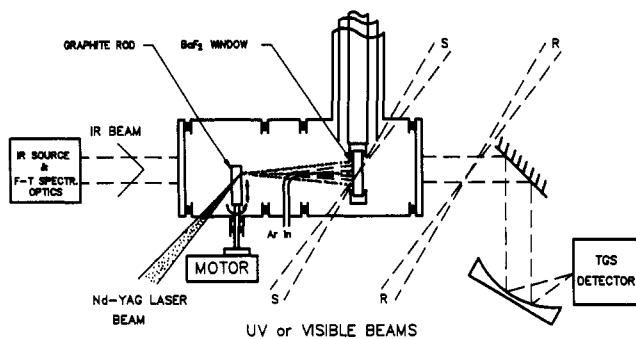


Figure 1. Vaporization/deposition cell showing low-temperature BaF₂ window through which IR beam and UV-visible sample (S) beam passes. The IR beam pathway contains KBr windows while the UV-visible S beam has quartz windows (not shown).

resolution in both spectral regions by using an FTIR spectrometer crossed with a double-beam optical spectrometer. Positive correlations between certain electronic bands and certain vibrational bands, the latter already ascribed to specific clusters, have been found and have permitted the definite assignment of several electronic bands.

II. Experimental Section

The carbon clusters were produced by the vaporization of graphite using a slightly focused Q-switched Nd:YAG laser (Spectra Physics, DCR-11). The ablated graphite products were trapped together with argon gas at 12 K on a BaF₂ window mounted in a copper holder on the cold finger of a closed-cycle helium cryostat (Displex 202, APD). The vaporization/deposition chamber is shown schematically in Figure 1. Deposition times were typically about 15 min with the laser beam (532 nm, 0.1 mJ/pulse, 10 Hz repetition rate) focused on the rotating graphite rod to a spot approximately 2 mm in diameter.

Interrogation by both IR and UV-visible beams on the same sample matrix was possible due to the crossed beam configuration used (cf. Figure 1). Infrared spectra were obtained on a Nicolet 7199 FT-IR spectrometer with 1 cm⁻¹ resolution (300 scans). The UV-visible spectra were measured by using a Cary 17 spectrophotometer with 0.2–0.6-nm resolution over the 210–600-nm range covered. A specially constructed sample compartment for the Cary 17 permitted the IR beam to exit the FT-IR spectrometer, pass through the BaF₂ sample window, and, using spherical and flat mirrors, focus on a TGS detector located below the sample cryostat. A glass tube connecting the FT-IR and UV-visible spectrometers permitted N₂ gas purging of the IR beam pathway from the IR source to the TGS detector in the special sample compartment. Other than the KBr windows used on the cryostat shroud and the BaF₂ used as the sample window, there were no absorptive elements in the light path. BaF₂ is transparent over the 210 nm to 14 μm range and is thus usable in both the IR and UV-visible regions.

In the annealing experiments the cryostat sample holder was heated stepwise from 12 K to a specified higher temperature (36 K maximum), after which the cryostat was cooled to 12 K and the UV-visible and IR spectra scanned sequentially. This sequence was then repeated for the next higher temperature.

III. Results

A. UV-Visible Bands. The temperature dependence of the UV-visible absorption bands due to matrix-isolated clusters of carbon obtained by laser vaporization is shown in Figure 2. These spectra were all scanned at 12 K, first immediately after deposition and then after annealing to temperatures of 23, 30, 33, and 36 K. The spectra are in good agreement (except for relative band intensities; vide infra) with spectra previously reported by Krättschmer, Sorg, and Huffman³ and by Kurtz and Huffman.⁴ Both sets of authors used resistively heated graphite rods for preparation of the carbon cluster samples, compared to our laser ablation method. No analysis of the vibrational structure or temperature behavior of the UV-visible bands observed has been

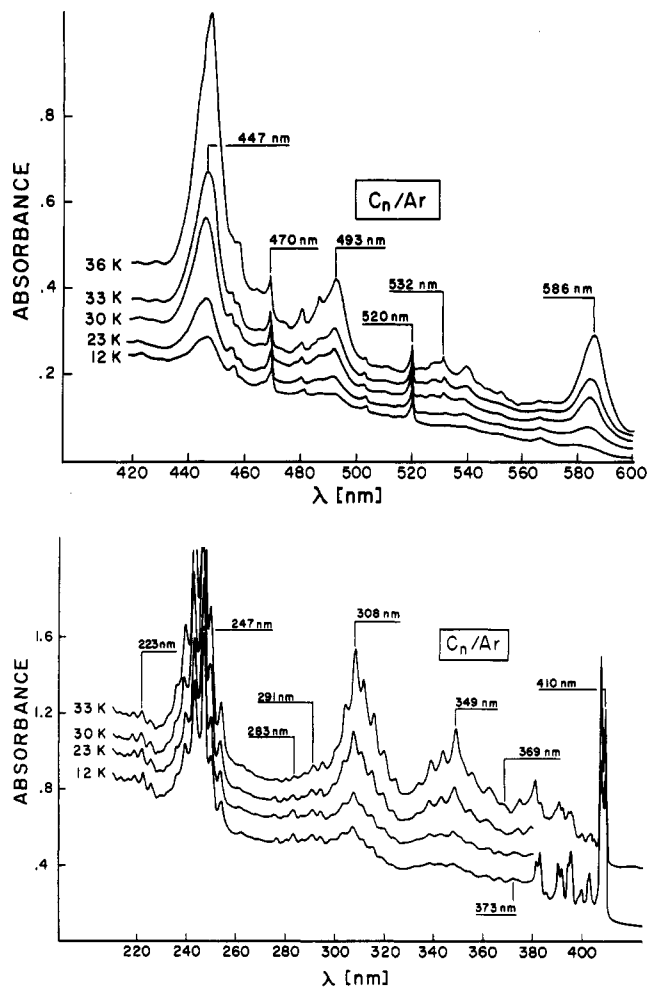


Figure 2. (a, top) Temperature dependence of visible spectrum of C_n clusters in an argon matrix. (b, bottom) Temperature dependence of UV spectrum of C_n clusters in an argon matrix. Marked peaks refer to important maxima given in Table I.

reported yet. Table I gives a tabulation of the various bands, their vibrational spacings, and the ratio of their band intensities at 36 and 12 K.

B. IR Bands. The temperature dependence of the infrared spectra corresponding to the above UV-visible spectra are shown in Figure 3. Only the range from 1600 to 2200 cm⁻¹ is shown since the largest temperature variations of the most prominent peaks corresponding to the carbon cluster stretching frequencies occur in this region. While the general features are roughly similar to the spectra reported by Kurtz and Huffman (KH),⁴ our higher resolution has permitted more bands to be observed. The effect of the different methods of preparation is reflected in the different relative intensities of some bands. For example, the ratio of the intensities of the 2164- and 2039-cm⁻¹ bands, due to linear C₅^{5,6} and C₃,² respectively, is greater in our spectra than in previous studies. Inspection of Figures 2 and 3 reveals that certain bands increase in intensity upon annealing while others decrease. Yet others appear to change little with annealing. The 2164-, 2039-, and 1544-cm⁻¹ IR peaks (latter not shown) all decrease with increasing temperature. Of the UV-visible bands, the 223-, 236.2-, 283.6-, and 410-nm bands behave in a similar fashion. On the other hand, the 1998-, 1700-, and 1695-cm⁻¹ bands increase with warming while the 2128- and 1952-cm⁻¹ peaks do not vary greatly with increasing temperature.

(5) Vala, M.; Chandrasekhar, T. M.; Szczepanski, J.; Pellow, R. *High Temp. Sci.* **1990**, *27*, 19.

(6) (a) Vala, M.; Chandrasekhar, T. M.; Szczepanski, J.; Van Zee, R.; Weltner, Jr., W. J. *Chem. Phys.* **1989**, *90*, 595. (b) Moazzen-Ahmadi, N.; McKellar, A. R. W.; Amano, T. *Chem. Phys. Lett.* **1989**, *157*, 1. (c) Heath, J. R.; Cooksey, A. L.; Gruebele, M. H. W.; Schuttenmaer, C. A.; Saykally, R. J. *Science* **1989**, *244*, 564.

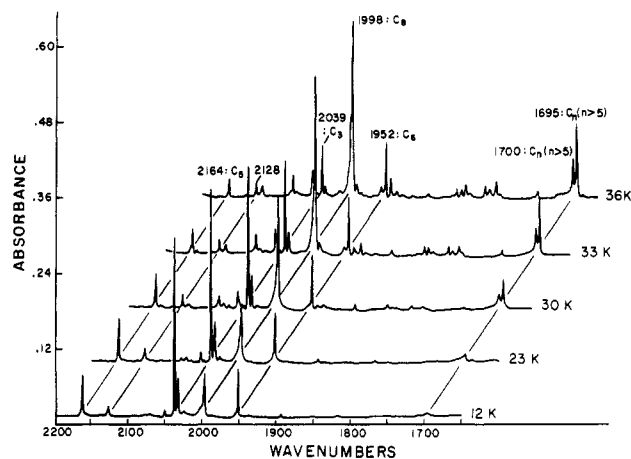


Figure 3. Temperature dependence of IR spectrum of the same C_n clusters whose UV-visible bands are shown in Figure 2. Each spectrum above 12 K is shifted an additional 50 cm^{-1} for clarity.

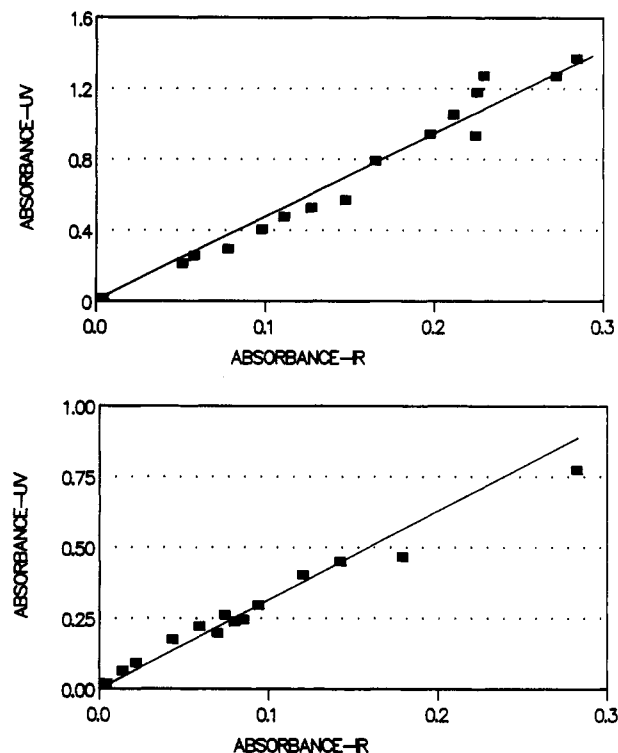


Figure 4. Correlation plots for the 410-nm/2039- cm^{-1} (top, a) and 308-nm/1998- cm^{-1} (bottom, b) UV-visible/IR band pairs.

C. Experimental Strategy. The approach taken in this work has been to find correlations in growth or decay patterns between IR and UV-visible bands upon annealing of the same sample matrix. Such a correlation, if found, represents a sufficient but not a necessary condition for the conclusion that the correlated bands belong to the same cluster. It is possible that similar growth (or decay) patterns could occur for two different species in the matrix. To establish a positive correlation it is necessary to perform experiments with different initial conditions, i.e., vary the initial concentration of the various clusters present. This can be accomplished by changing the ablation laser focus, matrix isolant gas deposition rate, etc. If a UV-visible band and an IR band do not originate from the same cluster species, changing initial conditions will change the relative concentrations of each species and the resulting correlation will be poor (vide infra).

D. Correlation of C_3 and C_8 UV-Visible and IR Bands. To illustrate the method used in the present work we focus initially on two bands whose correlations are already known. In recent work, KH found⁴ a good correlation for the 1998- cm^{-1} line and the 308-nm band, and attributed them to the near-linear C_8 cluster. Earlier work by Weltner and McLeod² established that the

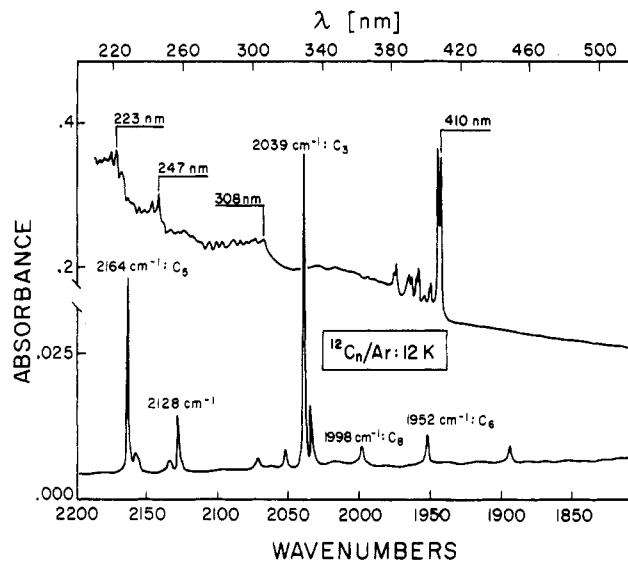


Figure 5. The UV-visible spectrum (top, a) and IR spectrum (bottom, b) of carbon products from defocused laser ablation.

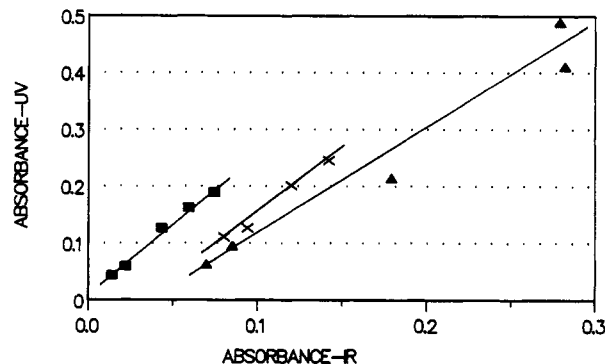


Figure 6. Correlation plot for the 349-nm/1998- cm^{-1} band pair.

2039- cm^{-1} and 410-nm band were due to the quasi-linear C_3 cluster.

Figure 4 shows our correlation plots for these two pairs. Each point represents the experimental IR and UV-visible band intensity for a particular matrix temperature (over the range 12–36 K) from three separate runs, each with different initial conditions. The relative initial IR intensities for C_3 : C_5 : C_6 : C_8 were 2.8:1.1:1.1:1.0 for the first run, 4.1:1.0:1.1:1.0 for the second run, and 13.0:6.6:1.5:1.0 for the third run, respectively. If the UV and IR bands belong to the same cluster species a straight line is expected. A good straight line is observed; the correlation coefficient for the 2039- cm^{-1} /410-nm plot is 0.98, while for the 1998- cm^{-1} /308-nm pair it is 0.99. We thus confirm the correlation between the 1998- cm^{-1} and 308-nm band found by KH.⁴

Inspection of Table I and Figure 2 reveals several interesting facts about the 308-nm band. First, the vibrational bands on the red edge of the band grow with annealing at a significantly greater rate than the bands on the blue edge of the band. The intensity ratios (36 K vs 12 K) of the former average 5.6, while for the latter they average only 3.8. Second, the vibrational spacings for the bands on the red edge are larger (433, 425, and 417 cm^{-1}) than those on the blue side (417 and 405 cm^{-1}). Interestingly, the vibrational bands on the blue edge of the lower energy 349-nm band show the same approximate vibrational spacing (434, 429, and 424 cm^{-1}) and same intensity ratio (6.0) as those on the red side of the 308-nm band. Finally, Figure 5 shows the result of an experiment in which the ablation laser was defocused to produce larger amounts of the smaller clusters. It can be seen that there are no vibrational bands observed to the red of the 308-nm peak. These observations lead us to conclude that the vibrational bands to the red of 308 nm belong to another electronic transition, most probably to another carbon cluster species. Furthermore, it appears likely that these bands form part of one vibrational pro-

TABLE I: Analysis of UV-Visible Bands for Carbon Clusters in an Argon Matrix

position of main band λ/nm	vibrational bands		vibrational interval $\Delta\bar{\nu}/\text{cm}^{-1}$	vibrational assignment ^a $\bar{\nu}/\text{cm}^{-1}$	intensity ratio $I_{36\text{K}}/I_{12\text{K}}$	cluster assignment, remarks			
	λ/nm	$\bar{\nu}/\text{cm}^{-1}$							
222.7	211.3	47 326	641	1813 + 2 × 654	0.44	linear C ₅			
	214.2	46 685	644	1813 + 654					
	217.2	46 041	483	1813					
	219.5	45 558	655	2 × 654					
	222.7	44 903	675	654					
	226.1	44 228		0					
247.1	236.3	42 319	609	1146 + 3 × 622	2.40	linear C ₉			
	239.7	41 710	609	1146 + 2 × 622					
	243.3	41 101	632	1146 + 622					
	247.1	40 469	509	1146					
	250.3	39 960	637	622					
	254.3	39 323		0					
283.6	280.5	35 651	390	390	~0.4	linear C ₃			
	283.6	35 261		0					
291.0	287.6	34 771	407	2 × 419	~2.0	linear C ₇ ?			
	291.0	34 364	431	419					
	294.7	33 933		0					
307.9	300.3	33 300	405	2 × 411	3.8	linear C ₈			
	304.0	32 895	417	411					
	307.9	32 478		0					
349.0	311.7	32 082	416	8 × 429	5.6				
	315.8	31 666	426	7 × 429					
	320.1	31 240	433	6 × 429					
	324.6	30 807	867	5 × 429					
	334.0	29 940	424	3 × 429					
	338.8	29 516	429	2 × 429					
	343.8	29 087	434	429					
	349.0	28 653		0					
	369.2	356.0	28 090	519			2 × 503	~4.5	
		362.7	27 571	486			503		
369.2		27 085		0					
373.0	367.6	27 203	393	393	<1	C ₃			
	373.0	26 810		0					
381.5	375.1	26 660	448	448	>1				
	381.5	26 212		0					
410.4	383.7	26 062			0.27	(1Π _u ← 1Σ _g ⁺)			
	386.7	25 860							
	392.7	25 465							
	403.7	24 768							
	410.4	24 366	<i>b</i>	<i>b</i>					
447.0	440.0	22 727	204	356	8.5	cyclic?			
	444.0	22 523	152	152					
	447.0	22 371		0					
519.9	469.3	21 308	2073	2073	1.6	C ₂ ⁻ ?			
	519.9	19 235		0					
493.0	481.5	20 768	234	2 × 242	>1	cyclic?			
	487.0	20 534	250	242					
	493.0	20 284		0					
532.0	532.0	18 797			>1				
586.0	586.0	17 065			~18-20	cyclic with <i>n</i> ≥ 6?			
616.0	616.0	16 234			>1				
639.0	639.0	15 649			>1				

^aVibrational frequencies are averages of all appropriate vibrational intervals from preceding column. ^bFor complete analysis, see: Weltner, Jr., W.; McLeod, Jr., *D. J. Chem. Phys.* **1964**, *40*, 1305.

gression (average spacing = 429 cm⁻¹) built on the 349-nm electronic band origin.

E. Noncorrelation of the 1998-cm⁻¹ and 349-nm Bands. KH observed that the temperature dependence of the 1998-cm⁻¹ line and the 349-nm band were very similar but concluded that they were not correlated.⁴ The results of our correlation runs for three different initial conditions are plotted in Figure 6. It can be seen that the data do not fall on one straight line, as seen above for

the 308-nm band. Indeed, if an extrapolation is made for two of the runs, a negative absorbance is predicted at low concentrations, a clearly nonphysical and unreasonable result. Furthermore, it appears this band is composed of two electronic transitions. The ratios of the intensities of the vibrational peaks over the whole band (327-370 nm) are not constant when the matrix is annealed. A constant ratio would be expected if the band were due to a single vibronic transition (cf. Figure 2). The energy

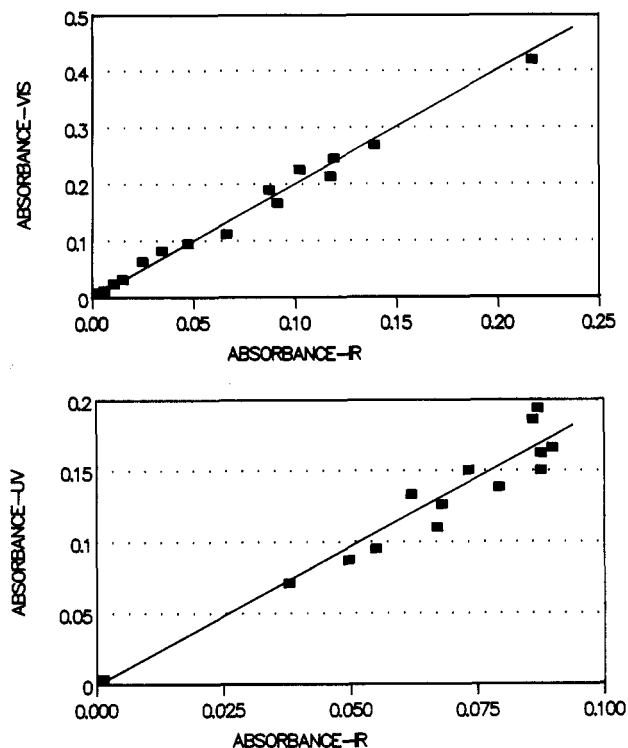


Figure 7. Correlation plot for the 586-nm/1695-cm⁻¹ (top, a) and 223-nm/2164-cm⁻¹ (bottom, b) band pairs.

spacing between vibrational peaks at the red edge of the band is ~ 503 cm⁻¹, while on the blue edge it is 429 cm⁻¹. We conclude that the broad band centered at 349 nm contains two (or possibly more) electronic transitions and that the 1998-cm⁻¹ IR band is not correlated to it. These transitions most likely do not belong to the C₈ cluster.

F. Correlation of the 1695-cm⁻¹ and 586-nm Bands. Figure 2 shows that the 586-nm visible band increases rapidly upon annealing. The 1695-cm⁻¹ band also grows dramatically with temperature annealing, as may be seen in Figure 3. The correlation of the 586-nm and the 1695-cm⁻¹ bands (cf. Figure 7a) is excellent (correlation coefficient = 0.99). The integrated intensity ratio of the 586-nm band to the 1695-cm⁻¹ line is 400. The 1700-cm⁻¹ line (cf. Figure 3) grows in a nearly parallel fashion with the 1695-cm⁻¹ feature. It is, however, difficult to decide whether this line is due to another cluster or the 1695-cm⁻¹ species in another stable matrix site. We favor the latter interpretation.

The 1695-cm⁻¹ band rises from a very small intensity at 12 K to a peak intensity approximately 20 times as intense at 36 K. In contrast, the 1998-cm⁻¹ band increases by a factor of only 4 from 12 to 36 K. We believe that there is a deeper lying significance to these intensity ratios than their mere numerical difference. For all the linear clusters known to date,⁷ the ratio of their growth rates (at 36 K compared to 12 K) are 4 or less. Yet some ratios for unassigned peaks are substantially greater, e.g., 20 for the 1695-cm⁻¹ band. From recent work⁷ on a new cluster/matrix aggregation model for linear clusters up to C₉, we have found that the growth ratios never become very large since there is a destruction route (i.e., aggregation) which limits the ultimate amount of each species formed. If this is so, how can we then explain the larger ratios observed here? We believe they arise from cyclic clusters, which could be formed by ring-closing of a linear species or by aggregation of two smaller clusters. Since their destruction rates would not be competitive with their formation rates, their growth rates could be quite rapid. For these reasons we surmise that the 1695-cm⁻¹ line belongs to a cyclic cluster containing six or more carbons. Interestingly, the 586-nm visible band, to which it is correlated, is quite broad and shows

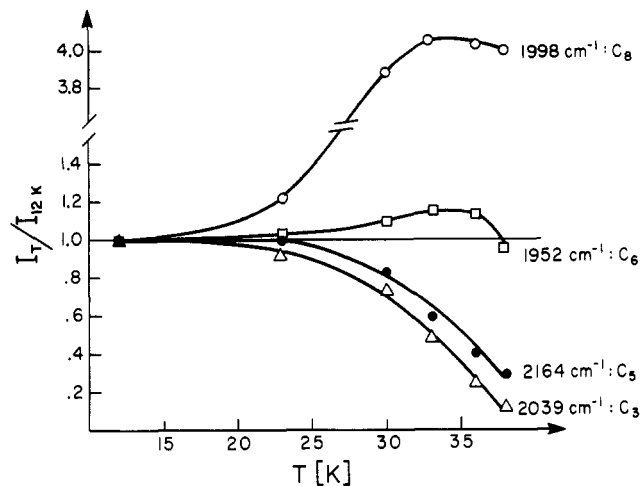


Figure 8. Temperature dependence of the peak heights of the 1998-cm⁻¹ (C₈), 1952-cm⁻¹ (C₆), 2164-cm⁻¹ (C₅), and 2039-cm⁻¹ (C₃) IR bands.

no vibrational structure. (This is in sharp contrast to the linear cluster electronic bands identified to date.) The identification of the cluster should be straightforward. Isotopic studies such as have already been done^{2,5,6} for C₃, C₅, and C₆ are planned for the near future.

G. Linear C₅ Ultraviolet Band. As noted above in section IIIB, the 2164-cm⁻¹ linear C₅ band decreases in intensity with matrix annealing. A number of UV bands were observed to also decrease with increasing temperature, viz., the 223-, 236.2-, and 283.6-nm bands. Correlation of the 2164-cm⁻¹ band with each of these UV bands was attempted. Only for the 223.0-nm band was a good correlation found (correlation coefficient = 0.96, cf. Figure 7b). We conclude that the 223-nm UV band is due to linear C₅. (The integrated intensity ratio of the entire band at 223 nm to the 2164-cm⁻¹ peak is 2000.)

To confirm this attribution the ablation laser was defocused significantly to produce predominantly smaller clusters upon deposition. The resultant IR and UV-visible scans are shown in Figure 5. Note that the relatively strong intensities for the 2164 cm⁻¹ (C₅) and 2039 cm⁻¹ (C₃) lines are mirrored in the UV-visible spectrum by the relatively strong bands at 223 nm (C₅) and 410 nm (C₃). Other species are present in smaller amounts, compared to the runs displayed in Figures 2 and 3.

In an earlier study⁶ on C₅ we observed that the 2164-cm⁻¹ band decreased in parallel with the 1544-cm⁻¹ band. From carbon isotope studies the 2164-cm⁻¹ line was ascribed to linear C₅ and by virtue of its similar temperature behavior the 1544-cm⁻¹ band was similarly attributed. (Because of its much lower relative intensity, isotopic results on the 1544 cm⁻¹ band were not seen by us.) Using a different approach Shen and Graham⁸ have recently succeeded in observing isotopic structure in this region and attribute the 1544-cm⁻¹ band to linear C₄. The question now arises: if the temperature dependence of the 2164-cm⁻¹ band parallels that of the 1544-cm⁻¹ one and the 2164-cm⁻¹ band correlates well with the 223-nm UV band, could the 223-nm band be due to C₄? No correlation, such as was done above, is possible between the 1544-cm⁻¹ and 223-nm bands because of the low intensity of the former. To answer the question, we resorted to a series of experiments in which the initial concentrations of the C₃, C₄, and C₅ clusters varied widely. The ratios of the 2164- and 1544-cm⁻¹ band intensities varied between 10 and 50 while at the same time the 2164- to the 2039-cm⁻¹ intensities changed between 0.2 and 0.5 for the same spectra. If the 223-nm band were due to C₄, with the very different ratios of C₄ and C₅ concentrations present in this series of runs, one would have expected the correlation of the 2164-cm⁻¹ line with the 223-nm band to be poor. It is, however, as noted above, quite good. The temperature dependence of the 2039- and 2164-cm⁻¹ bands are closely parallel (cf. Figure 8), yet the correlation between them is poor.

(7) Szczepanski, J.; Pellow, R.; Vala, M. *J. Chem. Phys.*, submitted for publication.

(8) Shen, L. N.; Graham, W. R. M. *J. Chem. Phys.* **1989**, *91*, 5115.

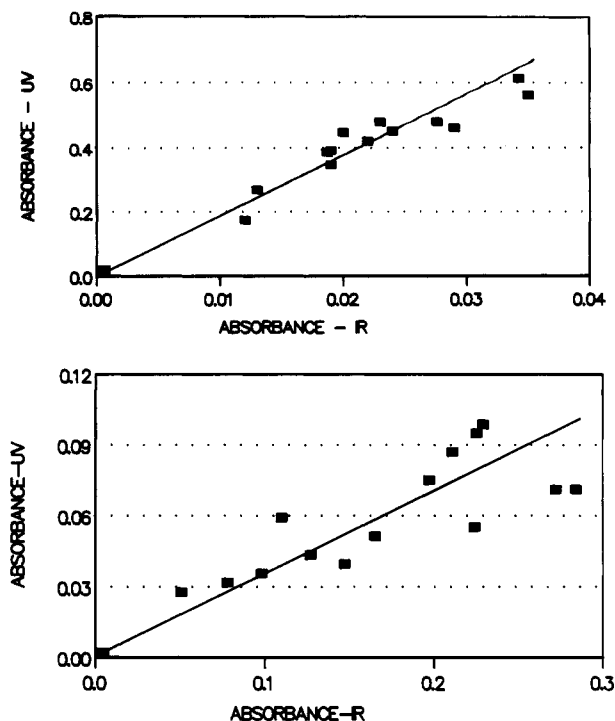


Figure 9. Correlation plots for the 247-nm/2004-cm⁻¹ (top, a) and the 283.6-nm/2039-cm⁻¹ (bottom, b) band pairs.

Thus the 223-nm UV band can be safely attributed to linear C₅.

The vibrational structure of the 223-nm band shows an interesting pattern (cf. Table I). Built on the origin at 226.1 nm (44 228 cm⁻¹) is a short two-member progression of average spacing 665 cm⁻¹ plus a one-member 1813-cm⁻¹ mode. On the latter band is also built a two-member progression in the 665-cm⁻¹ mode. These vibrational frequencies can be compared (with great caution, vide infra) to calculated values for linear C₅. Raghavachari and Binkley⁹ predict σ_g modes at 863 cm⁻¹ and 2220 cm⁻¹, while Kurtz and Adamowicz,¹⁰ and Martin, Francois, and Gijbels¹¹ both predict σ_g modes at 786 and 2018 cm⁻¹. Although this comparison is not strictly legitimate since the calculations are for the electronic ground state and the observed energies are for an excited state the values are in good agreement, particularly when the usually adopted scaling factor of approximately 0.9 is used on the theoretical values. This correspondence may signal that the electronic excitation does not greatly change the electronic distribution and hence leaves the force constants for these modes little perturbed.

H. Correlation of the 2004-cm⁻¹ and 247-nm Bands. The strong IR band at 1998 cm⁻¹ is actually composed of three bands which are readily discerned when the region is scanned under higher resolution (0.5 cm⁻¹ or better). The temperature dependence of these three components has been investigated by deconvoluting the observed band(s). The 1998- and 2000.5-cm⁻¹ bands display very similar temperature behavior; the 1998-cm⁻¹ band has been discussed above. The 2000.5-cm⁻¹ component may be a stable site or slightly different chain conformation of the C₃ cluster responsible for the 1998-cm⁻¹ feature. The correlation for the 2004-cm⁻¹ component with the 247.1-nm UV band is shown in Figure 9a. This plot represents three different runs with different initial cluster concentrations. Clearly the correlation is good (correlation coefficient = 0.93). The ratio of the 2004-cm⁻¹ peak intensity at 36 and 12 K is 2.6.

In related work, we have fit the temperature dependence of the known IR bands due to C₃, C₅, C₆, and C₈ to a new cluster/matrix aggregation model.⁷ All possible cluster formation and destruction steps have been included in the model for linear clusters up to

C₉. The many coupled differential equations have been solved and predictions made for the temperature dependence of the heretofore unknown species. Of importance here is the prediction for the linear C₉ cluster: it is expected to increase in abundance going from 12 to 36 K by a factor of 2.6. No other clusters are predicted to display this particular dependence. Because this ratio is the same as the observed ratio for the 2004-cm⁻¹ peaks, we conclude that both the 2004-cm⁻¹ band and the 247-nm UV band to which it is correlated arise from the linear or near-linear C₉ cluster.

I. Other Bands. It is worth commenting on several other bands that have been observed. A weak UV band at 283.6 nm, with a partner 390 cm⁻¹ higher, exhibited the same temperature dependence as the 2039-cm⁻¹ IR band due to C₃ (cf. Figure 9b for the correlation plot; correlation coefficient = 0.85). In their study of C₃ clusters, Weltner and McLeod² saw a weak band in a neon matrix at 281.2 nm but did not assign it. Kurtz and Huffman⁴ noted a weak band in argon at 283.5 nm and remarked that it paralleled the behavior of C₃ on annealing. Morse and co-workers¹² have studied jet-cooled C₃ and discovered a band system between 266 and 302 nm which they ascribe to either of the ¹Δ_u or ¹Π_g ← ¹Σ_g⁺ electric-dipole forbidden, vibronically allowed transitions. Given our good correlation of the 2039-cm⁻¹ IR band with the 283.6-nm UV band, it seems clear that the latter is due to C₃ and corresponds to the same band system seen by Morse and co-workers.

Another weak band system was observed at 373.0 nm with a higher energy partner at ~393 cm⁻¹. This band, which decreases with increasing annealing temperature, is severely overlapped by the blue-edge vibrational components of the 381.5-nm band, which increases strongly with annealing. It may be seen clearly only at the lower temperatures (up to ~25 K). This system is similar to the 283.6-nm band discussed above (same approximate temperature dependence and band spacing). We believe that both the 283.6- and 373.0-nm bands are due to C₃ and represent the two dipole-forbidden, vibronically allowed transitions predicted^{19,20} to lie in this region. The 390-cm⁻¹ bands are probably one quanta of the ν₂ bending mode which is known¹³ to increase dramatically in the C₃ electronically excited states. In the gas phase this mode jumps from 63 cm⁻¹ in the ground state to 308 cm⁻¹ in the excited state.¹³

Two strong, relatively broad visible bands have been observed at 493 and 447 nm. Both increase strongly with increasing matrix temperature (cf. Figure 2a). No correlations with any major IR peaks could be found. The widths of these bands and their growth rates are comparable to the 586-nm band discussed in section IIIF. There it was suggested that the 586-nm band might originate from a cyclic cluster containing six or more carbons. An analogous proposal is put forward here for the 493- and 447-nm bands.

A relatively weak peak at 291 nm exhibits no change with matrix annealing. No quantitative correlation was possible because of the small size of the peak. However, we have observed in another study⁷ that the 2128-cm⁻¹ IR band shows practically no variation with annealing temperature. On the basis of cluster aggregation kinetics a similar behavior was predicted⁷ for linear C₇. It was concluded that the 2128-cm⁻¹ band originated from linear C₇. From its similar temperature behavior we also tentatively ascribe the 291-nm band system to linear C₇.

IV. Discussion

In this paper evidence has been presented for the assignment of several UV-visible bands to the electronic transitions of specific carbon clusters. The 223-nm band has been ascribed to the linear C₅ cluster, the 247-nm band assigned tentatively to the linear C₉ cluster, the 308-nm band verified as due to chainlike C₈, the 368- and 283-nm bands designated to C₃, and the 586-nm band attributed to an unknown species, probably cyclic with n ≥ 6 carbons.

(9) Raghavachari, K.; Binkley, J. S. *J. Chem. Phys.* **1987**, *87*, 2191.

(10) Kurtz, J.; Adamowicz, L. *Astrophys. J.* **1990**, *370*.

(11) Martin, J. M. L.; Francois, J. P.; Gijbels, R. *J. Chem. Phys.* **1989**, *90*, 3403.

(12) Lemire, G. W.; Fu, Z.; Hamrick, Y. M.; Taylor, S.; Morse, M. D. *J. Phys. Chem.* **1989**, *93*, 2313.

(13) Gausset, L.; Herzberg, G.; Lagerqvist, A.; Rosen, B. *Discuss. Faraday Soc.* **1963**, *35*, 113; *Astrophys. J.* **1965**, *142*, 45.

While there has been much current theoretical activity directed toward the most stable ground-state geometries and their predicted infrared frequencies, there has been very little modern theoretical work performed on the properties of the excited electronic states of carbon clusters containing more than three carbon atoms (i.e., what are the locations, oscillator strengths, and polarizations of these transitions).

However, Pacchioni and Koutecký have calculated¹⁴ the expected excited electronic states of the linear and rhombic C₄ and linear C₅ species using ab initio single-reference and multireference configuration interaction calculations. For the C₅ cluster, three spin-forbidden excited states are predicted at about 2.5 eV. The first two spin-allowed transitions are expected at 3.18 eV (¹Π_u) and 6.76 eV (¹Σ_v⁺) with oscillator strengths of 1.6 × 10⁻² and 3.02, respectively. The latter represents a very strong transition. The Franck–Condon maximum in the observed band occurs at 222.7 nm (5.57 eV). This is in reasonable agreement with the calculated 6.76-eV value. We assign the 5.57-eV band to the ¹Σ_v⁺ ← ¹Σ_g⁺ transition.

The origin of the so-called 217.5-nm interstellar “hump” in the ultraviolet region has intrigued astrophysicists for years. It has usually been thought to result from a surface plasmon transition in small graphitic particles. There are, however, strong arguments against this interpretation.¹⁵ We propose here that the 217.5-nm feature is due to linear C₅ clusters. Several factors make this suggestion appealing. (1) Linear C₅ is known¹⁶ to exist in the cool outer shell of the carbon star, IRC+10216. It may be expected to appear in interstellar space also, since this carbon star (and presumably others) has lost (and is continuing to lose) substantial mass to interstellar space. (2) Linear C₅ has an ultraviolet absorption band in the correct position, with an almost symmetrical Franck–Condon envelope. If we account for the matrix-to-gas phase shift²³ (–5 nm), the Franck–Condon maximum would shift from 222.7 nm (matrix) to 217.7 nm (gas). (3) The band is an allowed electric dipole transition and is predicted to be very intense.¹⁴ For a bandwidth (fwhm) of 2500 cm⁻¹ (as observed in our matrix spectrum), the predicted¹⁴ oscillator strength of 3.02 translates into an extinction coefficient of 275 000 ! (4) Linear C₅ is not expected to have any bands of comparable intensity at lower energies. The predicted¹⁴ oscillator strength of the lower energy spin-allowed transition is only 0.016. (5) There are no known carbon clusters whose bands may interfere. The presence of C₃, thought^{16,17} to be 20 times more abundant than C₅ in the

circumstellar shell of IRC+10216, should not be visible since its lowest spin-allowed transition, ¹Π_u ← ¹Σ_g⁺, at 3.06 eV (410 nm), possesses an oscillator strength of only 0.0246. The higher lying allowed transition, the ¹Σ_v⁺ ← ¹Σ_g⁺, has been assigned by Chang and Graham¹⁸ to a band at 189 nm (6.6 eV), although several theoretical papers predict^{14,19,20} it to appear deeper in the UV region. Its predicted^{19,20} oscillator strength is 0.92. So, the C₃ bands are neither in the correct position nor of sufficient strength to account for the 217.5-nm interstellar feature. Theoretical results on the excited electronic states of carbon clusters other than C₃, C₄, and C₅ are unknown at present. Such studies appear to be worthwhile pursuing on this interesting class of clusters.

V. Conclusions

1. The 223-nm UV band has been assigned to linear C₅.
2. It is suggested that the 217.5-nm interstellar “hump” is perhaps due to the absorption of free linear C₅ clusters.
3. The correlation between the 308-nm UV band and the 1998-cm⁻¹ IR peak has been confirmed. These bands have been attributed to the near-linear C₈ cluster.
4. Two weak peaks at 283.6 and 373.0 nm have been identified with C₃. The transitions are most probably due to the two electric-dipole forbidden, symmetry-allowed bands expected in this region.
5. A good correlation has been established between the 1695-cm⁻¹ and 586-nm bands. It is suggested that the cluster responsible for these bands is cyclic with at least six carbons.
6. Two strong visible bands at 493 and 447 nm, for which IR correlations could not be found, are tentatively ascribed to cyclic carbon clusters.
7. A prominent band system at 247.1 nm has been tentatively attributed to linear C₉. A good correlation was found with the 2004-cm⁻¹ IR band. Further theoretical work on the excited electronic state properties of this and other small carbon clusters would greatly aid in the assignment of these bands.

Acknowledgment. We gratefully acknowledge stimulating conversations with Dr. Joseph Kurtz and Professor William Weltner. We also thank the National Science Foundation for its support of this research under Grant No. CHE-8903133.

Registry No. C, 7440-44-0; Ar, 7440-37-1; C₅, 12595-82-3; C₈, 107603-01-0; C₃, 12075-35-3.

(14) Pacchioni, G.; Koutecký, J. *J. Chem. Phys.* **1988**, *88*, 1066.

(15) Savage, B. D. *Astrophys. J.* **1975**, *199*, 92.

(16) Bernath, P. F.; Hinkle, K. H.; Keady, J. J. *Science* **1989**, *244*, 562.

(17) Botschwina, P.; Sebald, P. *Chem. Phys. Lett.* **1989**, *160*, 485.

(18) Chang, K. W.; Graham, W. R. *J. Chem. Phys.* **1982**, *77*, 4300.

(19) Römel, J.; Peyerimhoff, S. D.; Buenker, R. J. *Chem. Phys. Lett.* **1978**, *58*, 1.

(20) Williams, G. R. *J. Chem. Phys. Lett.* **1975**, *33*, 582.